PHYSICAL REVIEW B **99**, 134431 (2019)

Quasiperiodic magnetic chain as a spin filter for arbitrary spin states

Biplab Pal*
Max Planck Institute for the Physics of Complex Systems, Nöthnitzer Str. 38, 01187 Dresden, Germany

(Received 16 November 2018; revised manuscript received 8 January 2019; published 23 April 2019)

We show that a quasiperiodic magnetic chain comprising magnetic atomic sites sequenced in a Fibonacci pattern can act as a prospective candidate for spin filters for particles with arbitrary spin states. This can be achieved by tuning a suitable correlation between the amplitude of the substrate magnetic field and the on-site potential of the magnetic sites, which can be controlled by an external gate voltage. Such correlation leads to a spin filtering effect in the system, allowing one of the spin components to completely pass through the system while blocking the others over the allowed range of energies. The underlying mechanism behind this phenomena holds true for particles with any arbitrary spin states $S = 1, 3/2, 2, \ldots$, in addition to the canonical case of spin-half particles. Our results open up the interesting possibility of designing a spin demultiplexer using a simple quasiperiodic magnetic chain system. Experimental realization of this theoretical study might be possible by using ultracold quantum gases and can be useful in engineering new spintronic devices.

DOI: 10.1103/PhysRevB.99.134431

I. INTRODUCTION

The ability to controllably tune, manipulate and detect the spin degree of freedom of a particle in low-dimensional systems plays a pivotal role in the field of spintronics [1–3]. It has emerged as one of the most significant areas of research over the past few decades due to its potential to realize new functionalities in future electronic devices, and keep the promise to integrate memory and logic in a single device. Spin-based electronic devices are assumed to have several important advantages, such as high memory storage density, faster access speed, low power consumption, and nonvolatility, which give them a significant edge over the existing conventional electronic device technologies. To realize such devices for real-life applications, a detailed investigation and understanding of the spin-dependent transport in model nanostructured systems is of immense importance and can be treated as a powerful tool to envision the role of the spin degree of freedom in coherent electronic systems. Generation of a spin-polarized current source has been one of the key area of investigation in the spintronics research domain and has attracted intense theoretical as well as experimental research studies over the course of time [4–14].

For the desirable operations and the development of the spin-based devices such as spin-FETs [15], spin-interference devices [16], and readout devices for quantum information processing and quantum computers [17], the notion of spin-polarized current or the so-called spin filter is one of the most pertinent components. Spin interference effects in a quantum ring geometry subject to the Rashba spin-orbit interaction was successfully realized experimentally [18] a few years ago following an earlier theoretical study [19]. To date, some notable progress has been achieved in the study of spin-polarized transport, where people have used ferromagnetic semiconductor heterostructures [20,21], metallic multilayer structures [22], ferromagnetic metal-semiconductor interfaces [23], and carbon-based organic materials [11,12] among others to achieve highly controllable spin-polarized spin injection sources. Furthermore, the study of spin-polarized transport and spin filtering effects in quantum networks with loop geometries [24–27], or in helical molecules [28], and DNA double helix structure [29,30] has also ushered new light into this research arena, revealing different subtleties of spin polarized transport in mesoscopic systems.

However, to date, the study of spin-polarized transport has mainly focused on the transportation of electrons, i.e., for spin-1/2 particles, while the investigation of spin-polarized transport for particles with higher spin states, such as spin-1 or spin-3/2 or other higher-order states has not received the same level of attention. Only recently, the idea of spin-polarized transport and spin filtering effects for higher spin states in a periodic magnetic chain is being proposed and studied in detail [31]. We strongly believe that this is an area which needs to be explored more rigorously in order to bring out the possibilities of designing next-generation novel quantum information storage devices which rely on the spin-polarized transport of particles with arbitrary higher spin states. Such systems exhibiting higher-order spin states can be realized in experiments using ultracold fermionic or bosonic quantum gases [32–37].

It is always an intriguing question to ask whether one can have spin filtering phenomena in a system which has no long-range translational order. In the present article, we address this question and investigate the possibility of a spin filtering effect for arbitrary higher-order spin states in a quasiperiodic system. The quasiperiodic system we consider for our study is a Fibonacci chain, which represents the simplest model of a quasicrystal [38,39]. It is well known that the eigenstates of a periodic system are extended Bloch states [40] and the

*biplabpal@pks.mpg.de; biplabpal2008@gmail.com; Present address: Department of Physics, Ben-Gurion University, Beer-Sheva 84105, Israel.

corresponding energy spectrum is continuous while, for a disordered system, like in a one-dimensional Anderson model, all the eigenstates are localized [41]. In contrast to these two cases, for a Fibonacci quasiperiodic system, the energy spectrum forms a singular continuous Cantor set [38,39]. The corresponding eigenstates are critical and show multifractal character. Thus quasiperiodic systems, in general, are expected to show up poor conducting behavior. In this communication, we present a unique exception of the above scenario and show that, for a correlation between the parameters of the Hamiltonian, our simple tight-binding model of a quasiperiodic magnetic chain presents a ballistic transmission window for one of the spin channels while completely blocking the particles in the other spin channels. It is worth mentioning that, very recently, Mukherjee *et al.* have studied the spin filtering effect in a variety of aperiodic systems [42], where they have taken certain special kinds of quasi-one-dimensional building blocks to form the quasiperiodic systems. They have shown that, for some special numerical correlations between the hopping integrals of the system, and in some cases an additional external magnetic flux, will lead to a spin filtering effect in the system. We note that, in their study, in addition to a major spin channel having a high transmittivity, the other remaining minor spin channels also show some transport in their transmission characteristics. In contrast with the above scenario, we propose a very simple model of a one-dimensional quasiperiodic magnetic chain. Here one can only tune the values of the on-site potentials of the atomic sites by using some external gate voltages to accomplish a complete spin filtering effect for one of the desired spin components (channels), while the remaining spin components will have zero transport through the system under this condition.

In what follows, we present the model and describe the essential results. The layout of the paper is the following: In Sec. II, we introduce our model and describe the essential mathematical framework employed to extract the results. The results for the spin-dependent transport and the spin filtering effect along with the corresponding local density of states (LDOS) for different spin channels are discussed in detail in Sec. III. Finally, in Sec. IV, we draw our conclusion with a summary of the key findings and their possible applications.

II. THE MODEL AND THE THEORETICAL FRAMEWORK

A. The Fibonacci chain

We propose the construction of a linear magnetic chain model following a Fibonacci sequence. The Fibonacci sequence is a quasiperiodic sequence of two letters; say, $\mathcal{A}$ and $\mathcal{B}$. To construct the system, one can start from the letter $\mathcal{A}$, and then apply the following substitution rule to grow the system into its different higher-order generations:

$$\mathcal{A} \rightarrow \mathcal{AB} \text{ and } \mathcal{B} \rightarrow \mathcal{A}. \tag{1}$$

By using the above prescription in Eq. (1), we can easily construct the different generations of a Fibonacci system as follows: $\mathcal{ABA}$, $\mathcal{ABAAB}$, $\mathcal{ABAABABA}$, and so on. For our model, the letters $\mathcal{A}$ and $\mathcal{B}$ are simply replaced by two kinds of magnetic atomic sites grafted on some substrates to form the system shown in Fig. 1. These magnetic sites have magnetic moments $\vec{h}_\mathcal{A}$ and $\vec{h}_\mathcal{B}$, respectively, associated with them. In the thermodynamic limit, i.e., for an infinitely long chain, the ratio of $\mathcal{A}$-type to $\mathcal{B}$-type magnetic sites is incommensurate and gives $\sigma = (1+\sqrt{5})/2$, which is known as the "golden ratio."

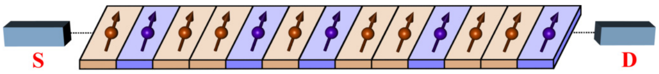

FIG. 1. Schematic diagram of a finite-size Fibonacci sequenced quasiperiodic magnetic layered structure coupled between two semi-infinite nonmagnetic leads, *viz.*, source (S) and drain (D).

B. Hamiltonian of the system

The Hamiltonian of the system in a tight-binding framework can be written as

$$\boldsymbol{H} = \sum_i \boldsymbol{c}_i^\dagger (\boldsymbol{\epsilon}_i - \vec{h}_i \cdot \vec{\boldsymbol{\mathcal{S}}}_i^{(S)})\boldsymbol{c}_i + \sum_{\langle i,j\rangle} (\boldsymbol{c}_i^\dagger \boldsymbol{t}_{ij} \boldsymbol{c}_j + \text{H.c.}), \tag{2}$$

where $\langle i, j\rangle$ indicates the nearest-neighbor atomic sites. We note that, each of the terms $\boldsymbol{c}_i^\dagger(\boldsymbol{c}_i)$, $\boldsymbol{\epsilon}_i$, $\boldsymbol{t}_{ij}$, and $\vec{\boldsymbol{\mathcal{S}}}_i^{(S)}$ represents multicomponent matrices with dimensions that depend on the spin of the particles. For the simplest case of a spin-half ($S = 1/2$) particle, these matrices, *viz.*, creation (annihilation) matrix, on-site potential matrix, and hopping matrix, take the following forms:

$$\boldsymbol{c}_i^\dagger = \begin{pmatrix} c_{i,\uparrow}^\dagger & c_{i,\downarrow}^\dagger \end{pmatrix}, \quad \boldsymbol{c}_i = \begin{pmatrix} c_{i,\uparrow} \\ c_{i,\downarrow} \end{pmatrix},$$
$$\boldsymbol{\epsilon}_i = \begin{pmatrix} \epsilon_{i,\uparrow} & 0 \\ 0 & \epsilon_{i,\downarrow} \end{pmatrix}, \quad \boldsymbol{t}_{ij} = \begin{pmatrix} t & 0 \\ 0 & t \end{pmatrix}, \tag{3}$$

where the indices "↑" and "↓" refer to the spin-*up* and spin-*down* components ("channels"), respectively. Note that the dimension of these matrices will increase proportionately as we go to the higher-order spin cases, *viz.*, $S = 1, 3/2, \ldots$, and so on. The term $\vec{h}_i \cdot \vec{\boldsymbol{\mathcal{S}}}_i^{(S)}$ represents the interaction of the spin (S) of the injected particle with the local magnetic field $\vec{h}_i \equiv (h_x, h_y, h_z)$ at site i. $\vec{\boldsymbol{\mathcal{S}}}_i^{(S)}$ represents the set of *generalized* Pauli spin matrices ($\boldsymbol{\mathcal{S}}_x, \boldsymbol{\mathcal{S}}_y, \boldsymbol{\mathcal{S}}_z$) expressed in units of $\hbar S$ for an incoming particle with spin S. For the spin-half ($S = 1/2$) case, ($\boldsymbol{\mathcal{S}}_x, \boldsymbol{\mathcal{S}}_y, \boldsymbol{\mathcal{S}}_z$) turns out to be the set of the usual Pauli spin matrices ($\boldsymbol{\sigma}_x, \boldsymbol{\sigma}_y, \boldsymbol{\sigma}_z$), and the term $\vec{h}_i \cdot \vec{\boldsymbol{\mathcal{S}}}_i^{(S)}$ at site i will have the following explicit form:

$$\vec{h}_i \cdot \vec{\boldsymbol{\mathcal{S}}}_i^{(S=1/2)} = \begin{pmatrix} h_i\cos\theta_i & h_i\sin\theta_i e^{-i\phi_i} \\ h_i\sin\theta_i e^{i\phi_i} & -h_i\cos\theta_i \end{pmatrix}, \tag{4}$$

where h_i is the amplitude of the vector $\vec{h}_i$, and θ_i and ϕ_i denote the polar and azimuthal angles, respectively, as shown in Fig. 2.

C. Equivalence of the spin system with a multi-strand ladder network

Using the Hamiltonian (2), one can write down the time-independent Schrödinger equation for a general spin-S system

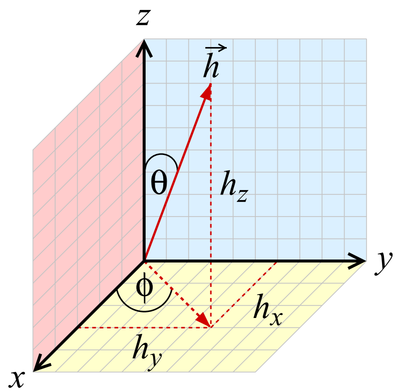

FIG. 2. Decomposition of $\vec{h}$ in a three-dimensional plane. θ denotes the polar angle and ϕ denotes the azimuthal angle.

as follows:

$$H|\Psi\rangle_S = E|\Psi\rangle_S, \text{ with } |\Psi\rangle_S = \sum_{\ell} \sum_{m_S=-S}^{+S} \psi_{\ell,m_S}|\ell, m_S\rangle. \quad (5)$$

A simplification of Eq. (5) for a spin-half ($S = 1/2$) system will lead to the following set of difference equations corresponding to the spin-*up* (↑) and spin-*down* (↓) channels, respectively, as follows:

$$[E - (\epsilon_{i,\uparrow} - h_i \cos\theta_i)]\psi_{i,\uparrow} + h_i \sin\theta_i e^{-i\phi_i}\psi_{i,\downarrow} = t\psi_{i+1,\uparrow} + t\psi_{i-1,\uparrow}, \quad (6a)$$

$$[E - (\epsilon_{i,\downarrow} + h_i \cos\theta_i)]\psi_{i,\downarrow} + h_i \sin\theta_i e^{i\phi_i}\psi_{i,\uparrow} = t\psi_{i+1,\downarrow} + t\psi_{i-1,\downarrow}. \quad (6b)$$

It is interesting to note that the above set of difference equations (6a) and (6b) resemble the difference equations for a spinless particle in a two-strand ladder network [43]. The effective on-site potentials for the *upper* strand (identified with the spin-*up* (↑) component) and the *lower* strand (identified with the spin-*down* (↓) component) of the analogous ladder network are $\epsilon_{i,\uparrow} - h_i \cos\theta_i$ and $\epsilon_{i,\downarrow} + h_i \cos\theta_i$, respectively, the hopping amplitude between the two neighboring sites along each strand of the ladder can be identified as t, while the term $h_i \sin\theta_i e^{i\phi_i}$ plays the role of the interstrand coupling along the ith rung of the ladder.

In a similar way, starting from Eq. (5) for a spin-1 ($S = 1$) system, we can obtain the following set of three coupled difference equations for the three spin channels 1, 0, and −1, respectively, as

$$[E - (\epsilon_{i,1} - h_i \cos\theta_i)]\psi_{i,1} + \frac{1}{\sqrt{2}}h_i \sin\theta_i e^{-i\phi_i}\psi_{i,0} = t\psi_{i+1,1} + t\psi_{i-1,1}, \quad (7a)$$

$$[E - \epsilon_{i,0}]\psi_{i,0} + \frac{1}{\sqrt{2}}h_i \sin\theta_i e^{i\phi_i}\psi_{i,1} + \frac{1}{\sqrt{2}}h_i \sin\theta_i e^{-i\phi_i}\psi_{i,-1} = t\psi_{i+1,0} + t\psi_{i-1,0}, \quad (7b)$$

$$[E - (\epsilon_{i,-1} + h_i \cos\theta_i)]\psi_{i,-1} + \frac{1}{\sqrt{2}}h_i \sin\theta_i e^{i\phi_i}\psi_{i,0} = t\psi_{i+1,-1} + t\psi_{i-1,-1}, \quad (7c)$$

where we have used the following set of spin matrices ($\boldsymbol{\mathcal{S}}_x^{S=1}, \boldsymbol{\mathcal{S}}_y^{S=1}, \boldsymbol{\mathcal{S}}_z^{S=1}$) for a spin-1 system:

$$\boldsymbol{\mathcal{S}}_x^{S=1} = \frac{1}{\sqrt{2}}\begin{pmatrix} 0 & 1 & 0 \\ 1 & 0 & 1 \\ 0 & 1 & 0 \end{pmatrix}, \quad \boldsymbol{\mathcal{S}}_y^{S=1} = \frac{1}{\sqrt{2}}\begin{pmatrix} 0 & -i & 0 \\ i & 0 & -i \\ 0 & i & 0 \end{pmatrix}, \quad \boldsymbol{\mathcal{S}}_z^{S=1} = \begin{pmatrix} 1 & 0 & 0 \\ 0 & 0 & 0 \\ 0 & 0 & -1 \end{pmatrix}. \quad (8)$$

Once again, the above prescription leads to the fact that a spin-1 ($S = 1$) system can be identified with a three-strand ladder network for a spinless particle. The above two analyses for the spin-half ($S = 1/2$) and the spin-1 ($S = 1$) cases lead to the conclusion that the above treatment can be extended to a general spin-S system and can be identified with an equivalent $(2S + 1)$ strand ladder model for spinless particles. We note that, as we go to the higher-order spin cases, there will be more such coupled difference equations corresponding to the different spin channels. This analogy between the spin model and the multi-strand ladder network is employed to engineer the spin filtering effect for our quasiperiodic system, as described in the subsequent sections.

III. RESULTS AND DISCUSSION

One of the essential requirements to have the spin filtering effect is to decouple the different spin channels from each other, i.e., there should not be any spin mixing between different spin components. For our model, this condition can be satisfied by setting the polar angle $\theta_i = 0 \ \forall \ i$. By looking at the set of equations (6) and (7), it can be easily understood that the hybridization terms (spin-mixing terms) between different spin components vanishes for $\theta_i = 0$ as the $\sin\theta_i$ terms vanishes under this condition, irrespective of the value of the azimuthal angle ϕ_i. The physical meaning of the above condition is that the magnetic moments of the atomic sites in the system have to be aligned along the z axis parallel to each other.

A. Spin-half ($S = 1/2$) system

For a spin-half ($S = 1/2$) system, the above choice of θ_i will lead to the following set of equations from Eq. (6):

$$[E - (\epsilon_{i,\uparrow} - h_i)]\psi_{i,\uparrow} = t\psi_{i+1,\uparrow} + t\psi_{i-1,\uparrow}, \quad (9a)$$

$$[E - (\epsilon_{i,\downarrow} + h_i)]\psi_{i,\downarrow} = t\psi_{i+1,\downarrow} + t\psi_{i-1,\downarrow}. \quad (9b)$$

It is apparent from the two equations above that the spin-*up* (↑) and the spin-*down* (↓) channels are now completely decoupled from each other. We furthermore can choose $\epsilon_{i,\uparrow} = \epsilon_{i,\downarrow} = \epsilon_i$, i.e., the on-site energies at an ith atomic site are to be the same for both the spin-up (↑) and the spin-down (↓) particles. For our model, h_i can take two possible values $h_\mathcal{A}$ and $h_\mathcal{B}$ sequenced following a Fibonacci pattern, as depicted in Fig. 1. Such a sequence can be generated mathematically by using

$$h_i = P + Q[\lfloor(i+1)(\sigma-1)\rfloor - \lfloor i(\sigma-1)\rfloor], \tag{10}$$

where the function $\lfloor x \rfloor$ denotes the greatest integer less than x, $\sigma = (1+\sqrt{5})/2$, and P and Q are two parameters that control the values of $h_\mathcal{A}$ and $h_\mathcal{B}$. Using Eq. (10), one can easily find that the values of $h_\mathcal{A}$ and $h_\mathcal{B}$ will turn out to be $h_\mathcal{A} = P + Q$ and $h_\mathcal{B} = P$, respectively, sequenced in a Fibonacci pattern. We can also choose the values of the on-site potentials ϵ_i to follow a Fibonacci pattern, consisting of two kinds of constituents $\epsilon_\mathcal{A}$ and $\epsilon_\mathcal{B}$, respectively. The values of these two on-site potentials can be easily controlled by using an external gate voltage [5]. Hence, one can easily have the exactly identical Fibonacci pattern for ϵ_i as that of h_i.

Now with this convention, if we set $\epsilon_\mathcal{A} = \Delta + h_\mathcal{A}$ and $\epsilon_\mathcal{B} = \Delta + h_\mathcal{B}$ (where Δ is some constant value which sets the center of the energy spectrum), then from Eq. (9), it immediately follows that, for the spin-*up* (↑) channel, the effective on-site potentials on different atomic sites will have a constant value, while for the spin-*down* (↓) channel the effective on-site potentials on different atomic sites will follow a Fibonacci quasiperiodic pattern. As a result of this, we will have an absolutely continuous energy spectrum for the spin-*up* (↑) channel populated with extended states, while the spin-*down* (↓) channel will feature a singular continuous multifractal spectrum. Thus, under this condition, we will have a high transmission probability for the spin-*up* (↑) particles whereas the spin-*down* (↓) particles will encounter zero transmission probability. To analyze this fact, we evaluate the local density of states (LDOS) for the different spin channels by using the Green's function technique. The formula for the LDOS is

$$\rho_{j,m_S} = -\frac{1}{\pi} \lim_{\eta\to 0^+} [\mathrm{Im}(\langle j, m_S|\boldsymbol{G}(E)|j, m_S\rangle)], \tag{11}$$

where $\boldsymbol{G}(E) = (z^+\boldsymbol{I} - \boldsymbol{H})^{-1}$ is the Green's function with $z^+ = E + i\eta$ ($\eta \to 0^+$), and m_S will have $2S+1$ values for a general spin-S system, e.g., for the spin-half ($S = 1/2$) case, $m_S = 1/2(\uparrow), -1/2(\downarrow)$.

We show the plots of LDOS for the spin-*up* (↑) and the spin-*down* (↓) channels in Fig. 3(a). We have used a real-space renormalization group (RSRG) method [44,45] to compute the LDOS spectrum for the different spin channels. We can clearly observe that the spin-*up* (↑) channel shows an absolutely continuous energy spectrum in between $E = \Delta - 2t$ and $E = \Delta + 2t$ (here we have taken $\Delta = 0$ and $t = 1$). All the eigenstates populated under this absolutely continuous energy spectrum are of extended character. For the spin-*down* (↓) channel, we have a multifractal energy spectrum with self-similarity, which exhibits the signature of a quasiperiodic system. The corresponding transmission probabilities for the two spin channels, *viz.*, up (↑) and down (↓), are exhibited in Fig. 3(b). Evidently, we have a high transmission probability $T_\uparrow$ for the spin-*up* (↑) component corresponding to the

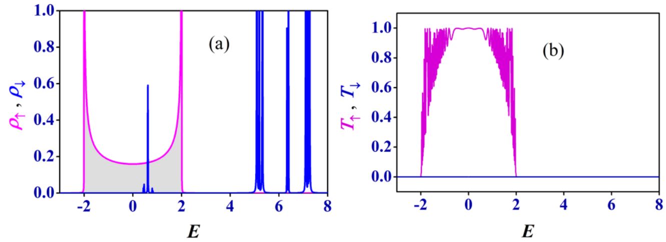

FIG. 3. (a) Plots of LDOS for the spin-*up* (↑) and the spin-*down* (↓) channels under the correlation condition $\epsilon_\mathcal{A} = \Delta + h_\mathcal{A}$ and $\epsilon_\mathcal{B} = \Delta + h_\mathcal{B}$. The spin-*up* (↑) channel exhibits an absolutely continuous spectrum (shaded portion) while the spin-*down* (↓) channel shows a multifractal singular continuous spectrum. We set $\Delta = 0$, $h_\mathcal{A} = 3$, and $h_\mathcal{B} = 0.5$ measured in units of the hopping integral t. (b) The corresponding transmission probabilities $T_\uparrow$ and $T_\downarrow$ for the spin-*up* (↑) and the spin-*down* (↓) components computed for a 15th-generation Fibonacci magnetic chain with 610 atomic sites.

absolutely continuous spectrum in Fig. 3(a), while the spin-*down* (↓) component gets completely blocked with zero transmission probability $T_\downarrow$. To evaluate these transmission characteristics, we take a finite-size quasiperiodic magnetic chain and couple it in between two nonmagnetic periodic leads, *viz.*, source (S) and drain (D), as shown schematically in Fig. 1. For the results of the transmission probabilities presented here, we have considered a 15th generation Fibonacci chain with 610 atomic sites. The values of the other parameters; namely, the on-site potentials for the atomic sites in the leads, the hopping amplitudes for sites in the lead, and the lead to magnetic chain (MC) couplings are chosen to be $\epsilon_S = \epsilon_D = 0$, $t_S = t_D = 4$, and $t_{S,MC} = t_{MC,D} = 4$, respectively, for our calculation. We have used a standard transfer-matrix method (TMM) elaborated in detail in Ref. [31] to obtain the transmission probabilities corresponding to the different spin components for our quasiperiodic system.

We note that one can have exactly the opposite phenomenon as compared with the results described in the last two paragraphs for a different choice of correlation between the two sets of parameters $\{\epsilon_\mathcal{A}, \epsilon_\mathcal{B}\}$ and $\{h_\mathcal{A}, h_\mathcal{B}\}$, *viz.*, $\epsilon_\mathcal{A} = \Delta - h_\mathcal{A}$ and $\epsilon_\mathcal{B} = \Delta - h_\mathcal{B}$, where Δ is a constant value which sets the center of the energy spectrum. With this choice of the correlation, it follows from Eq. (9) that now we will have a constant value of the effective on-site energies for the spin-*down* (↓) channel whereas the particles in the spin-*up* (↑) channel will feel a quasiperiodic effective on-site potential. Consequently, we will have an absolutely continuous energy spectrum for the spin-*down* (↓) channel and a multifractal self-similar singular continuous spectrum for the spin-*up* (↑) channel as shown in Fig. 4(a). The resulting transmission characteristics for this case are displayed in Fig. 4(b), where we can clearly see that the particles with spin-*down* (↓) component will have a transparent transmitting window for the allowed energy regime while the particles with spin-*up* (↑) component will have a completely opaque transmitting window. So the conclusion is that one can make a tunable spin filter for one of the desired spin components by choosing an appropriate correlation between $\{\epsilon_\mathcal{A}, \epsilon_\mathcal{B}\}$ and $\{h_\mathcal{A}, h_\mathcal{B}\}$. This can be achieved basically by suitably tuning the values of $\epsilon_\mathcal{A}$ and $\epsilon_\mathcal{B}$ using some external gate voltages. The typical

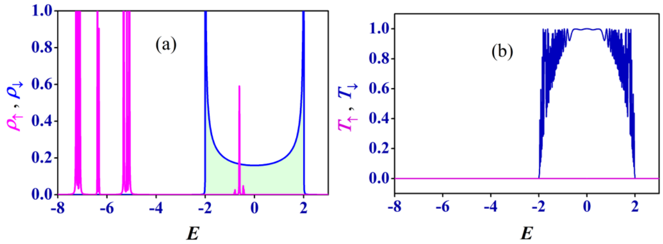

FIG. 4. (a) Plots of LDOS for the spin-*up* (↑) and the spin-*down* (↓) components with the correlation condition $\epsilon_{\mathcal{A}} = \Delta - h_{\mathcal{A}}$ and $\epsilon_{\mathcal{B}} = \Delta - h_{\mathcal{B}}$. We choose $\Delta = 0$, $h_{\mathcal{A}} = 3$, and $h_{\mathcal{B}} = 0.5$ measured in units of the hopping integral t. (b) The corresponding transmission characteristics $T_{\uparrow}$ and $T_{\downarrow}$ measured for a 15th generation Fibonacci magnetic chain containing 610 atomic sites. The other parameters are same as in Fig. 3.

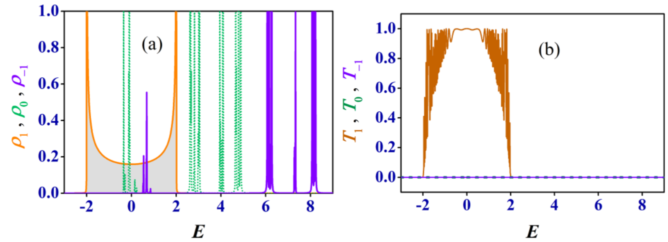

FIG. 5. (a) Plots for the LDOS for the spin-1, spin-0 and spin-(−1) components with the correlation condition $\epsilon_{\mathcal{A}} = \Delta + h_{\mathcal{A}}$ and $\epsilon_{\mathcal{B}} = \Delta + h_{\mathcal{B}}$. We take $\Delta = 0$, $h_{\mathcal{A}} = 3.5$, and $h_{\mathcal{B}} = 0.5$ measured in units of the hopping integral t. (b) The corresponding transmission probabilities T_1, T_0, and T_{-1} evaluated for a 15th generation Fibonacci magnetic chain containing 610 atomic sites. The lead parameters are $\epsilon_S = \epsilon_D = 0$, $t_S = t_D = 5$, and $t_{S,MC} = t_{MC,D} = 4$, respectively. The plots with the dotted lines in both panels are for the spin-0 component.

experimental value of the spatial extension over which a modulation of the gate voltage can be achieved is in the range of 100–150 nm.

B. Spin-1 ($S = 1$) system

Now we turn to the case of a spin-1 ($S = 1$) system, which has three components, *viz*., 1, 0, and −1. It can be identified with a $2S + 1 = 3$ strand ladder network. Once again, by setting the polar angle $\theta_i = 0\ \forall\ i$, we can decouple the three spin channels from each other, and analyze the transport properties for each of these three different spin channels. With the above choice, the three decoupled equations following from Eq. (7) can be written as

$$[E - (\epsilon_{i,1} - h_i)]\psi_{i,1} = t\psi_{i+1,1} + t\psi_{i-1,1}, \tag{12a}$$

$$[E - \epsilon_{i,0}]\psi_{i,0} = t\psi_{i+1,0} + t\psi_{i-1,0}, \tag{12b}$$

$$[E - (\epsilon_{i,-1} + h_i)]\psi_{i,-1}+ = t\psi_{i+1,-1} + t\psi_{i-1,-1}. \tag{12c}$$

Now we can choose $\epsilon_{i,1} = \epsilon_{i,0} = \epsilon_{i,-1} = \epsilon_i$, i.e., the values of the on-site potentials for the three different spin components at an ith atomic site are assumed to be the same. We know that, for our model, the values of the local magnetic fields $h_i = h_{\mathcal{A}}$ and $h_{\mathcal{B}}$, are distributed following a Fibonacci pattern. We can choose exactly the same Fibonacci sequence for the values of the on-site potentials $\epsilon_i = \epsilon_{\mathcal{A}}$ and $\epsilon_{\mathcal{B}}$. We can then suitably control the values of $\epsilon_{\mathcal{A}}$ and $\epsilon_{\mathcal{B}}$ through some external gate voltages to have the appropriate correlation condition for the spin filtering. The possible correlation conditions for the spin-1 particles are $\epsilon_i = \Delta \pm h_i,\ \ i \in \{\mathcal{A}, \mathcal{B}\}$. By applying one of these two sets of conditions, we generate an absolutely continuous energy spectrum for one of the three spin channels while the remaining channels will have multifractal energy spectrum. Consequently, we will have one of the spin components passing through the system while the remaining ones will be completely blocked. In Fig. 5, we exhibit one such situation as a prototype example, where we apply the correlation conditions $\epsilon_{\mathcal{A}} = \Delta + h_{\mathcal{A}}$ and $\epsilon_{\mathcal{B}} = \Delta + h_{\mathcal{B}}$. This makes the system completely transparent for the particles with spin-1 component, while completely impeding the particles with spin-0 and spin-(−1) components. It is easily understood that the other correlation condition will make the spin-(−1) component transparent through the system while blocking the particles with spin-0 and spin-1 components. We do not show this result to save space. We note that we cannot have spin filtering for the spin-0 component; as for the spin-0 channel, we do not have an "h term" in the effective on-site potentials, as reflected in Eq. (12b).

C. Other higher-order spin systems

It can be appreciated that the mathematical framework we have used to compute the results for the previous two cases of a spin-half ($S = 1/2$) and a spin-1 ($S = 1$) system can be easily extended for any general "spin-S" system. It is automatically understood that, as we go to the higher-order spin cases, we will have more numbers of spin components and eventually one of them will filter out through the system for the suitable correlations between the values of the local magnetic fields and the on-site potentials. Of course, we need to have different choices of correlations between ϵ_i and h_i to achieve the spin filtering for different cases as we move up along the higher-order spin ladder. We note that, to have the filtering for a particle with a certain spin component, the Fermi energy of the particle has to lie within a certain energy range where the absolutely continuum spectrum appears. One can easily work out that, for the case spin $S = 3/2$, the set of correlation conditions will be $\epsilon_i = \Delta \pm h_i$ and $\epsilon_i = \Delta \pm (h_i/3)$; for the case spin $S = 2$, the set of correlation conditions will be $\epsilon_i = \Delta \pm h_i$ and $\epsilon_i = \Delta \pm (h_i/2)$; and for the case spin $S = 5/2$, the set of correlation conditions will be $\epsilon_i = \Delta \pm h_i$, $\epsilon_i = \Delta \pm (h_i/5)$, and $\epsilon_i = \Delta \pm (3h_i/5)$. Here $i \in \{\mathcal{A}, \mathcal{B}\}$ for our Fibonacci quasiperiodic magnetic chain model. One can also calculate the conditions for the spin filtering for other higher-order spin particles following the same prescription.

Remark on the various disorder effects on the spin filtering phenomenon. It is important to discuss the robustness of the spin filtering protocol with respect to various disorder effects in the system. One can easily understand that disorder or thermal fluctuations in the system will spoil the perfect alignment of the polar angles $\theta_i = 0\,\forall\,i$ of the magnetic moments. Hence, it is significant to understand what should be the cutoff limit in the random tilting of the θ_i angles before the spin filtering mechanism in the system breaks down. Upon performing a rigorous numerical investigation, it has been found that our results on the spin filtering effect are fairly robust for small random tilting of the angle θ_i below $\theta_i = \pm 10$ degrees. Beyond this critical value of random tilting of θ_i, the states populating the energy spectrum consist of highly localized states, directing the system to act as a poorly conducting system. So it can be concluded that, for a weak disorder (or thermal broadening) corresponding to the above-mentioned critical value of random tilting of the angle θ_i, the spin filtering protocol persists.

Similarly, it is also worth addressing the effect of the mismatches between the on-site energies ϵ_i and the local magnetic fields h_i at different atomic sites on the spin filtering effect. One can capture this effect by choosing a random Δ_i. We have numerically found that, for a very weak random disorder in Δ_i, chosen randomly between the values $-0.2t$ and $0.2t$ (t being the hopping amplitude), the spin filtering effect is preserved in the system. As we increase the strength of this disorder to higher values, strong localization effect starts to take over and the efficiency of the spin transport through the system is extensively reduced. So the protocol for the spin filtering in our system is robust against weak disorder in Δ_i. It is also to be noted that, for larger S the system could be more inclined towards thermal fluctuations. But in an actual experimental situation, such thermal fluctuations can be controlled by performing the experiment at a low temperature. However, we have to keep in mind that, from the point of view of practical applicability, one cannot go down too low in the temperature scale. Hence, for a real-life application purpose one has to judiciously compromise between the thermal fluctuations and the temperature scale.

IV. CONCLUSION

In this paper, we have studied the spin-dependent transport for particles with arbitrary higher-order spin states in a tight-binding quasiperiodic magnetic chain model. A mathematical analogy between a multi-strand ladder network for spinless particles and a multicomponent spin-S system mimicking a $(2S + 1)$ strand ladder network has been exploited to analyze the problem and extract the useful results for the spin filtering for different spin components. We show that, by incorporating a suitable correlation between the magnitude of the of local magnetic fields and the on-site potentials of the magnetic atomic sites, one can render an absolutely continuous energy spectrum for one of the desired spin channels (components) with a highly transmitting window for the entire allowed energy range, while the other spin channels exhibit a multifractal energy spectrum with zero transmission probabilities. We show and explain the results in detail for two prototype examples of spin-half ($S = 1/2$) and spin-1 ($S = 1$) cases. We also give the outline for the other higher-order spin cases and justify that the essential mathematical exercise employed by us for our problem is a general one that holds true for any arbitrary higher-order spin-S particles, where S is an integer or half-integer.

Some of the recent interesting experimental studies [46,47] show that it is possible to manipulate the spin direction of individual magnetic atoms to form nanomagnets with arrays of a few exchange-coupled atomic magnetic moments, exhibiting a rich variety of magnetic properties and can be explored as the constituents of nanospintronic technologies. This indicates that our theoretical proposal of a quasiperiodic magnetic chain with an array of atomic magnetic moments sequenced in a Fibonacci pattern is not far from reality and might be realized in real-life experiments. Our results can be useful to realize novel magnetic quantum information storage devices and spin-based logic operators [48], relying on the operation of higher-order spin states. One can carry forward our analysis and results of this work for systems with other quasiperiodic sequences like Thue–Morse, period-doubling, copper mean, etc. Finally, we believe that our theoretical study of the realization of spin filters by using a simple tight-binding quasiperiodic magnetic chain system might open up an interesting futuristic prospect of realizing spin filters using quasicrystalline materials.

ACKNOWLEDGMENTS

The author gratefully acknowledges the funding and the facilities provided by MPIPKS through a postdoctoral scholarship. The author would like to thank A. Mukherjee and T. Nag for some useful suggestions on the manuscript. The author would also like to express his appreciation for the valuable suggestions and constructive criticisms of the anonymous referees in preparing the revised manuscript.

[1] G. Prinz, Science **282**, 1660 (1998).

[2] S. A. Wolf, D. D. Awschalom, R. A. Buhrman, J. M. Daughton, S. von Molnár, M. L. Roukes, A. Y. Chtchelkanova, and D. M. Treger, Science **294**, 1488 (2001).

[3] S. Sahoo, T. Kontos, J. Furer, C. Hoffmann, M. Gräber, A. Cottet, and C. Schönenberger, Nat. Phys. **1**, 99 (2005).

[4] T. Koga, J. Nitta, H. Takayanagi, and S. Datta, Phys. Rev. Lett. **88**, 126601 (2002).

[5] J. A. Folk, R. M. Potok, C. M. Marcus, and V. Umansky, Science **299**, 679 (2003).

[6] L. P. Rokhinson, V. Larkina, Y. B. Lyanda-Geller, L. N. Pfeiffer, and K. W. West, Phys. Rev. Lett. **93**, 146601 (2004).

[7] S. K. Watson, R. M. Potok, C. M. Marcus, and V. Umansky, Phys. Rev. Lett. **91**, 258301 (2003).

[8] P. Recher, E. V. Sukhorukov, and D. Loss, Phys. Rev. Lett. **85**, 1962 (2000).

[9] A. A. Kiseleva and K. W. Kim, Appl. Phys. Lett. **78**, 775 (2001).

[10] P. LeClair, J. K. Ha, H. J. M. Swagten, J. T. Kohlhepp, C. H. van de Vin, and W. J. M. de Jonge, Appl. Phys. Lett. **80**, 625 (2002).

[11] M. Koleini, M. Paulsson, and M. Brandbyge, Phys. Rev. Lett. **98**, 197202 (2007).

[12] M. G. Zeng, L. Shen, Y. Q. Cai, Z. D. Sha, and Y. P. Feng, Appl. Phys. Lett. **96**, 042104 (2010).

[13] P. Chuang, S.-C. Ho, L. W. Smith, F. Sfigakis, M. Pepper, C.-H. Chen, J.-C. Fan, J. P. Griffiths, I. Farrer, H. E. Beere, G. A. C. Jones, D. A. Ritchie, and T.-M. Chen, Nat. Nanotechnol. **10**, 35 (2015).

[14] W. Yan, O. Txoperena, R. Llopis, H. Dery, L. E. Hueso, and F. Casanova, Nat. Commun. **7**, 13372 (2016).

[15] S. Datta and B. Das, Appl. Phys. Lett. **56**, 665 (1990).

[16] J. Nitta, F. E. Meijer, and H. Takayanagi, Appl. Phys. Lett. **75**, 695 (1999).

[17] *Semiconductor Spintronics and Quantum Computation*, edited by D. Awschalom, D. Loss, and N. Samarth (Springer, New York, 2002).

[18] F. Nagasawa, J. Takagi, Y. Kunihashi, M. Kohda, and J. Nitta, Phys. Rev. Lett. **108**, 086801 (2012).

[19] D. Frustaglia and K. Richter, Phys. Rev. B **69**, 235310 (2004).

[20] R. Fiederling, M. Keim, G. Reuscher, W. Ossau, G. Schmidt, A. Waag, and L. W. Molenkamp, Nature (London) **402**, 787 (1999).

[21] Y. Ohno, D. K. Young, B. Beschoten, F. Matsukura, H. Ohno, and D. D. Awschalom, Nature (London) **402**, 790 (1999).

[22] Y. Tserkovnyak, A. Brataas, and G. E. W. Bauer, Phys. Rev. B **66**, 224403 (2002).

[23] P. R. Hammar, B. R. Bennett, M. J. Yang, and M. Johnson, Phys. Rev. Lett. **83**, 203 (1999); P. R. Hammar and M. Johnson, *ibid.* **88**, 066806 (2002).

[24] M. Popp, D. Frustaglia, and K. Richter, Nanotechnol. **14**, 347 (2003).

[25] D. Bercioux, M. Governale, V. Cataudella, and V. M. Ramaglia, Phys. Rev. Lett. **93**, 056802 (2004).

[26] A. Aharony, O. Entin-Wohlman, Y. Tokura, and S. Katsumoto, Phys. Rev. B **78**, 125328 (2008).

[27] B. Pal and P. Dutta, Sci. Rep. **6**, 32543 (2016).

[28] T.-R. Pan, A.-M. Guo, and Q.-F. Sun, Phys. Rev. B **92**, 115418 (2015).

[29] A.-M. Guo and Q.-F. Sun, Phys. Rev. Lett. **108**, 218102 (2012).

[30] B. Göhler, V. Hamelbeck, T. Z. Markus, M. Kettner, G. F. Hanne, Z. Vager, R. Naaman, and H. Zacharias, Science **331**, 894 (2011).

[31] B. Pal, R. A. Römer, and A. Chakrabarti, J. Phys.: Condens. Matter **28**, 335301 (2016).

[32] T.-L. Ho and S. Yip, Phys. Rev. Lett. **82**, 247 (1999).

[33] P. Lecheminant, E. Boulat, and P. Azaria, Phys. Rev. Lett. **95**, 240402 (2005).

[34] M. Fattori, T. Koch, S. Goetz, A. Griesmaier, S. Hensler, J. Stuhler, and T. Pfau, Nat. Phys. **2**, 765 (2006).

[35] A. V. Gorshkov, M. Hermele, V. Gurarie, C. Xu, P. S. Julienne, J. Ye, P. Zoller, E. Demler, M. D. Lukin, and A. M. Rey, Nat. Phys. **6**, 289 (2010).

[36] S. Taie, R. Yamazaki, S. Sugawa, and Y. Takahashi, Nat. Phys. **8**, 825 (2012).

[37] G. Pagano, M. Mancini, G. Cappellini, P. Lombardi, F. Schäfer, H. Hu, X.-J. Liu, J. Catani, C. Sias, M. Inguscio, and L. Fallani, Nat. Phys. **10**, 198 (2014).

[38] M. Kohmoto, L. P. Kadanoff, and C. Tang, Phys. Rev. Lett. **50**, 1870 (1983).

[39] C. Tang and M. Kohmoto, Phys. Rev. B **34**, 2041(R) (1986).

[40] C. Kittel, *Introduction to Solid State Physics*, 8th ed. (Wiley, New York, 2005).

[41] P. W. Anderson, Phys. Rev. **109**, 1492 (1958).

[42] A. Mukherjee, A. Chakrabarti, and R. A. Römer, Phys. Rev. B **98**, 075415 (2018).

[43] S. Sil, S. K. Maiti, and A. Chakrabarti, Phys. Rev. B **78**, 113103 (2008).

[44] B. Pal and A. Chakrabarti, Physica E (Amsterdam, Neth.) **60**, 188 (2014).

[45] B. Pal and A. Chakrabarti, Phys. Lett. A **378**, 2782 (2014).

[46] D. Serrate, P. Ferriani, Y. Yoshida, S.-W. Hla, M. Menzel, K. von Bergmann, S. Heinze, A. Kubetzka, and R. Wiesendanger, Nat. Nanotechnol. **5**, 350 (2010).

[47] A. A. Khajetoorians, J. Wiebe, B. Chilian, S. Lounis, S. Blügel, and R. Wiesendanger, Nat. Phys. **8**, 497 (2012).

[48] A. A. Khajetoorians, J. Wiebe, B. Chilian, and R. Wiesendanger, Science **332**, 1162 (2011).